Journal Pre-proofs

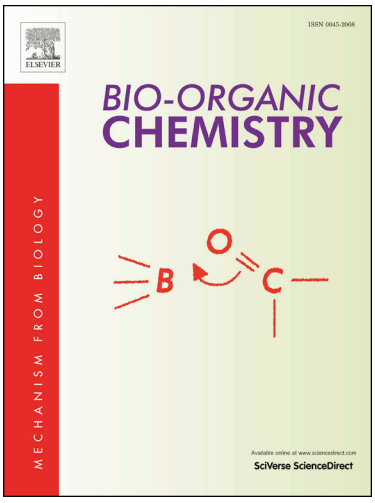

Synthesis, characterization, *in vitro* tissue-nonspecific alkaline phosphatase (TNAP) and intestinal alkaline phosphatase (IAP) inhibition studies and computational evaluation of novel thiazole derivatives

Hamid Aziz, Abid Mahmood, Sumera Zaib, Aamer Saeed, Zahid Shafiq, Julie Pelletier, Jean Sévigny, Jamshed Iqbal

PII: S0045-2068(20)31385-7
DOI: https://doi.org/10.1016/j.bioorg.2020.104088
Reference: YBIOO 104088

To appear in: *Bioorganic Chemistry*

Received Date: 8 April 2020
Revised Date: 3 July 2020
Accepted Date: 7 July 2020

Please cite this article as: H. Aziz, A. Mahmood, S. Zaib, A. Saeed, Z. Shafiq, J. Pelletier, J. Sévigny, J. Iqbal, Synthesis, characterization, *in vitro* tissue-nonspecific alkaline phosphatase (TNAP) and intestinal alkaline phosphatase (IAP) inhibition studies and computational evaluation of novel thiazole derivatives, *Bioorganic Chemistry* (2020), doi: https://doi.org/10.1016/j.bioorg.2020.104088

Synthesis, characterization, *in vitro* tissue-nonspecific alkaline phosphatase (TNAP) and intestinal alkaline phosphatase (IAP) inhibition studies and computational evaluation of novel thiazole derivatives

Hamid Aziz[a], Abid Mahmood[b], Sumera Zaib[b], Aamer Saeed[a]* Zahid Shafiq[c] Julie Pelletier[c], Jean Sévigny[c,d], Jamshed Iqbal[b*]

[a]*Department of Chemistry Quaid-I-Azam University Islamabad, 45320 Pakistan*

[b]*Centre for Advanced Drug Research, COMSATS University Islamabad, Abbottabad Campus, Abbottabad-22060, Pakistan.*

[c]*Institute of Chemical Sciences, Bahauddin Zakariya University, Multan-60800 Pakistan*

[d]*Centre de Recherche du CHU de Québec – Université Laval, Québec, QC, G1V 4G2, Canada.*

[e]*Département de microbiologie-infectiologie et d'immunologie, Faculté de Médecine, Université Laval, Québec, QC, G1V 0A6, Canada.*

[*]**Corresponding authors:** e-mail address: aamersaeed@yahoo.com; drjamshed@cuiatd.edu.pk;

Address: Department of Chemistry Quaid-I-Azam University Islamabad, 45320 Pakistan [Prof. Dr. Aamer Saeed]; Centre for Advanced Drug Research, COMSATS University Islamabad, Abbottabad Campus, Abbottabad-22060, Pakistan [Prof. Dr. Jamshed Iqbal]

Highlights

- New thiosemicarbazides (**3a-3e)** were heterocyclized with 1,3-dicarbonyls to afford thiazoles (**5a-f**) and with phenacyl halides to furnish the thiazoles (**5g-l**).
- The functionalized thiazoles (**5a-l**), were subjected to *h*-TNAP and *h*-IAP assay and **5e** and **5f** were identified as most active molecules.
- Molecular docking of **5e** and **5f** on *h*-TNAP and *h*-IAP to explore the binding interactions was carried out
- Molecular dynamic simulations were carried out to investigate the overall stability of protein in apo and holo state.

Graphical abstract:

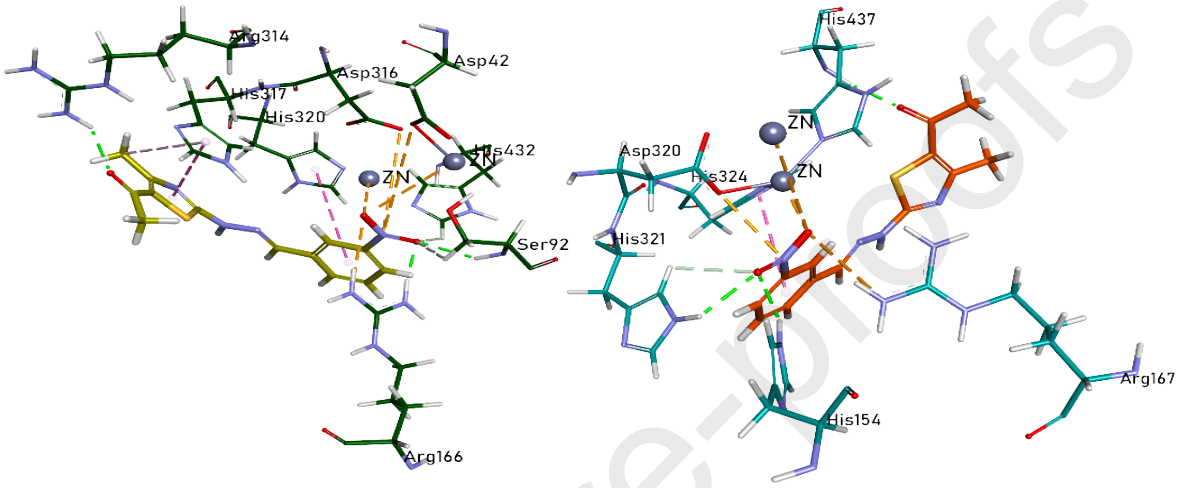

Binding interactions of compound ***5e*** in *h*-IAP (left) and compound ***5e*** *h*-TNAP (right) showing competitive mode of inhibition in both the enzymes

Abstract

Alkaline phosphatases (APs) are a class of homodimeric enzymes which physiologically possess the dephosphorylation ability. APs catalyzes the hydrolysis of monoesters into phosphoric acid which in turn catalyze a transphosphorylation reaction. Thiazoles are nitrogen and sulfur containing aromatic heterocycles considered as effective APs inhibitors. In this context, the current research paper presents the successful synthesis, spectroscopic characterization and *in vitro* alkaline phosphatase inhibitory potential of new thiazole derivatives. The structure activity relationship and molecular docking studies were performed to find out the binding modes of the screened compounds with the target site of tissue non-specific alkaline phosphatase (*h*-TNAP) as well as intestinal alkaline phosphatase (*h*-IAP). Compound **5e** was found to be potent inhibitor of *h*-TNAP with IC_{50} value of 0.17±0.01 µM. Additionally, compounds **5a** and **5i** were found to be highly selective toward *h*-TNAP with IC_{50} values of 0.25±0.01 µM and 0.21±0.02 µM, respectively. In case of *h*-IAP compound 5f was the most potent inhibitor with IC_{50} value of 1.33±0.10 µM. The most active compounds were resort to molecular docking studies on *h*-TNAP and *h*-IAP to explore the possible binding interactions of enzyme-ligand complexes. Molecular dynamic simulations were carried out to investigate the overall stability of protein in apo and holo state.

Key words: Thiazole; Structure Activity Relationship; Tissue Specific Alkaline Phosphatase; Hydrogen Bonding. Xx

1. Introduction

Enzymes are macromolecular proteins used as biological catalysts in fundamental as well as clinical research. Alkaline phosphatases (APs, EC 3.1.3.1) from the family of ectonucleotidases are dimeric enzymes having two Zn-atoms, one Mg-atom and five cysteine residues [1-3]. APs are found in blood serum from bone (50-60%), intestinal (30%) and hepatic (10-20%) fractions [4]. APs hydrolyze O/S-phosphorothioates, phosphoramidates, thiophosphates, phosphate and oxyphosphate monoesters into phosphate at alkaline pH. They are categorized as tissue specific (placental, germ cells, intestinal) and tissue non-specific isozymes found in kidneys, bones and central nervous system [5]. Intestinal alkaline phosphatases (*h*-IAPs) are found on the border of intestine and regulated lipid absorption, bicarbonate secretion, maintain pH at duodenum surface and controls bacterial endotoxins inflammation. The *h*-IAPs perform the detoxification of intestinal lipopolysaccharide and maintain homeostasis. Human tissue non-specific alkaline phosphatases (*h*-TNAP) hydrolyze inorganic pyrophosphate to phosphate and regulate mineral deposition in bones. APs facilitate the absorption of nutrients across cell membranes and serve as a mediator in physiological processes to regulate cellular functions including metabolism, gene expression, molecular transportation and signal transduction. The isozymes increase the concentration of inorganic phosphate and decreases the extracellular pyrophosphate [6,7]. The deficiency of *h*-IAPs cause inflammation owing to the insufficient detoxification of commensal bacteria. Similarly, the increase in APs cause disproportionate intracellular fat depots and mineralization disorders. This in turn damage musculoskeletal system and induces metabolism related disorders which ultimately damages liver and kidney cells. Thus, the selective inhibition and effective regulation of APs isozymes are required to develop useful therapies against osteoarthritis, rickets, arterial calcification and myocardial infection. In this regard, literature survey reveals heterocyclic analogues particularly 1,3-thiazoles as potent inhibitors of APs isozyme [8-9].

Thiazoles are five-member aromatic heterocycles containing sulfur and nitrogen atoms at 1,3-positions. Thiazoles are isomeric with 1, 2-azoles, containing sulfur and nitrogen atoms at 1,2-positions termed as isothiazole [10]. Thiazoles are easily metabolized by biological reactions and are non-carcinogenic in nature. Thiazole, a prime component of vitamin B_1, are essential scaffolds in pharmaceuticals, functional organic materials, asymmetric ligands and agrochemicals [11]. Among the biologically active natural products, thiazoles have been found to display diverse biological potential including antimicrobial [12], anticancer [13], anticonvulsant [14], neuroprotective analgesic [15], antioxidant and anti-inflammatory [16]. Thiazole core skeleton is present in many drugs including Tiazofurin (antineoplastic), Nitazoxanide (antiparasitic), Nizatidine (antiulcer), Thiamethoxam (insecticide), Fentiazac and Meloxicam (anti-inflammatory) as shown in Figure 1. Triazolothiadiazoles possess significant potential as APs inhibitors and some of the investigated thiazole analogues are proven to be more potent inhibitors than the reference drugs [17].

Thus, keeping in view the physiological profile of AP isozymes, and the diverse pharmacological potential of thiazole core and their ability to effectively inhibit the APs isozymes, the synthesis of functionalized thiazoles is required. In this regard, the current research reports the facile synthesis, spectroscopic characterization, APs inhibition assay and molecular modelling studies of thiazolyl ethanone derivatives the thiazolyl hydrazine [18]. The synthesis is performed in an efficient way using dry ethanol as a solvent and a catalytic amount of concentrated sulphuric acid.

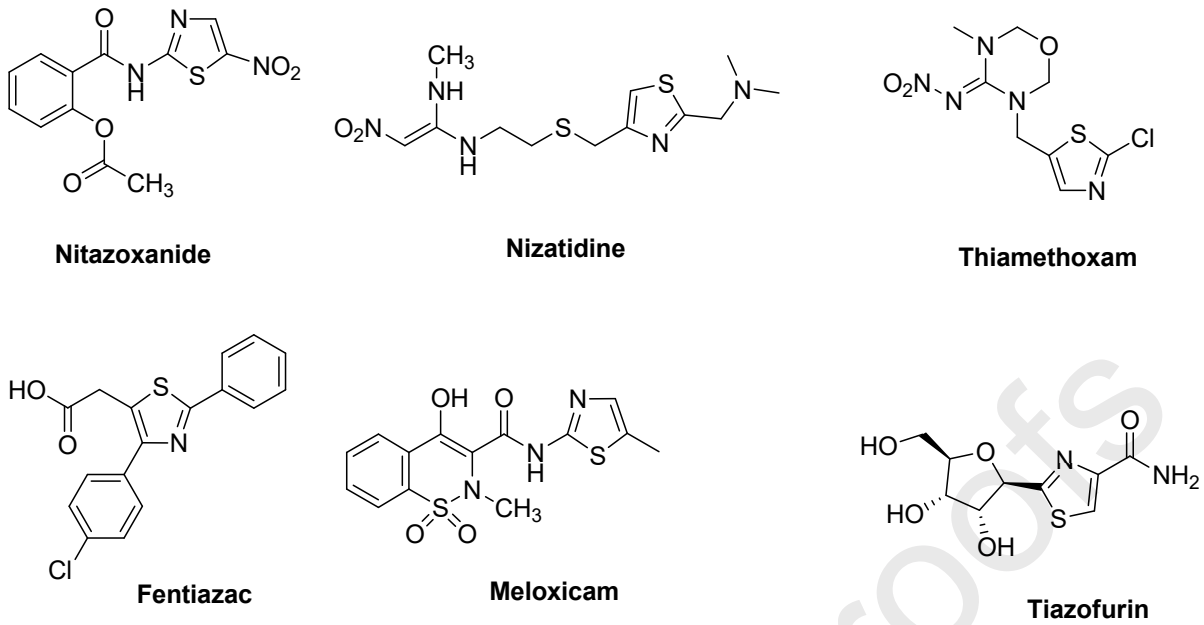

Figure 1. Some literature reported potent thiazole based drugs

2. Results and discussion

2.1. Synthesis of thiazole derivatives (5a-l)

The synthetic pathyway employed for the synthesis of the target thiazolyl ethanone **(5a-f)** and thiazolyl hydrazine derivatives **(5g-l)** is displayed in Scheme 1. Thus, the common semicarbazones as key intermediates **(3a-e)**, were obtained by the acid catalysed condensation of suitably substituted benzaldehydes with thiosemicarbazide in dry ethanol. The thiazolyl ethanone derivatives **(5a-f)** were obtained by reaction of **(3a-e)**, with 1,3-dicarbonyl compounds **(4a)** in dry ethanol in the absence of any catalyst under reflux conditions. A similar reaction of substituted phenacyl halides **(4b)** with intermediates **(3a-e)** afforded the thiazolyl hydrazines **(5g-l)**. All compounds were recrystallized from ethanol at room temperature to afford the pure products in high purity and good to excellent yields (scheme 1).

2.2. Characterization

The structures of the intermediates **(3a-e)**, thiazolyl ethanone derivatives **(5a-f)** and as well as the thiazolyl hydrazines **(5g-l)** were established through elemental analysis (CHNS) and spectroscopic techniques (FT-IR, ^{1}H and ^{13}C NMR). The C, H, N and S analyzer provided percent data highly aligned with the elements present in the synthesized compounds.

The FT-IR spectrum of a typical thiosemicarbazone **(3e)** showed the stretchings for NH_2 at 3238, for NH 3178, 1620 for HC=N and 1159.67 cm^{-1} for C=S, while rest of signals appeared at their respective regions. Compound **(3e)** exhibited the NH protons as characteristic broad singlets at 10.20 and 7.90 and at 8.45 for OH, whilst the presence of HC=N at 8.43 ppm in the ^{1}H NMR spectrum was noted. The thiocarbonyl C=S appeared at 181.43 and C=N carbons at 143.30 C=N ppm in the ^{13}C NMR spectrum.

The stretchings for NH at 320, 3098, 2958 for (C=C-H), 2914.23, 2840.29 for CH_3, 1625.73 for HC=N were observed in In the FT-IR spectrum of a typical thiazolyl ethanone (**5a**). Similarly, the ^{1}H NMR displayed broad singlet for 11.08 for NH, singlet at 8.10 for H-C=N, and 3.88 singlet for methyl of thiazole ring and 3.74 for methyl of carboxylate moiety. In ^{13}C NMR absence of thiocarbonyl and appearance of signals at 170.52 for C=N, 166.34 (C=O), 143.43 (C=N ring) and at 10.26, 28.49 for methyl of thiazole ring and carboxylate respectively was noted.

The thiazolyl hydrazine **(5h)** showed stretchings for 3276 (NH), 2987 (C=C-H), 1623 (HC=N), cm^{-1} FT-IR spectrum and broad singlets at 11.20 for NH, characteristic 1H singlet at 8.20 for HC=N, another at 6.64 for C=C-H, besides those for aromatic protons were noted in ^{1}H NMR. The important signals of ^{13}C NMR include those at δ 171.80 (C=N), 146.50 (C=C), 143.22 (HC=N) ppm.

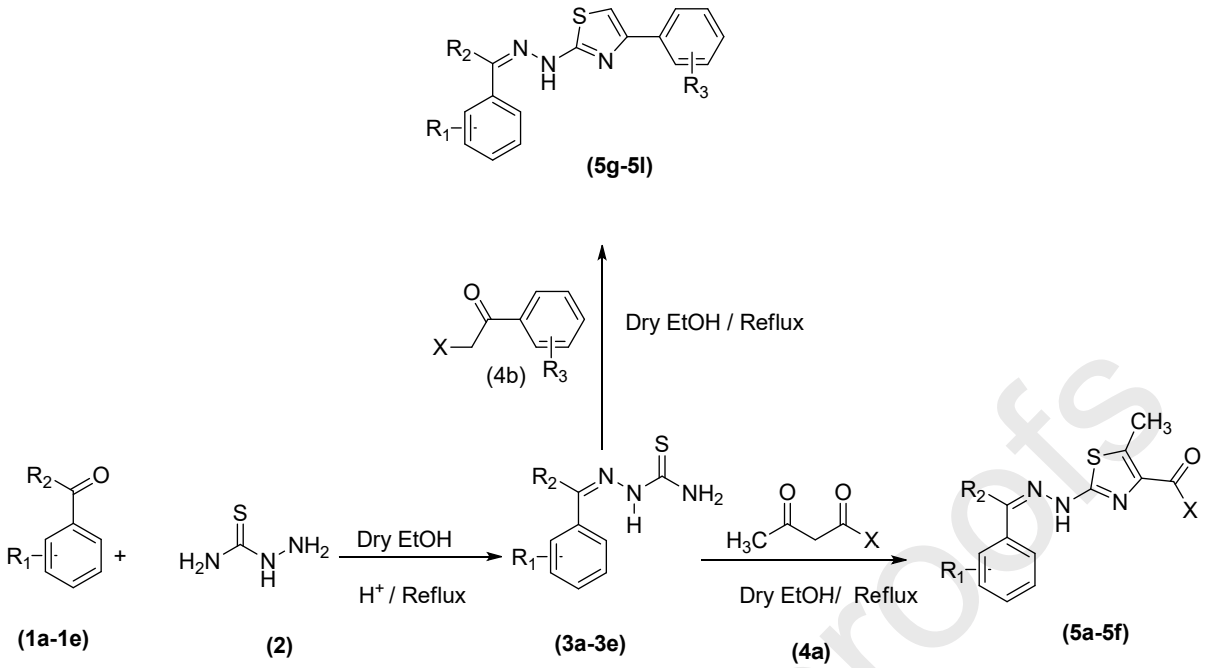

Scheme 1. Synthetic route employed for the thiazole derivatives **(5a-l)**

The different substituents attached to the synthesized thiazole derivatives **(5a-l)** are listed in Table-1.

Table 1. Structures of the synthesized thiazole derivatives **(5a-l)**

Compound	R_1	R_2	X	Compound	R_1	R_2	R_3
5a	3-OCH_3,4-OH	H	OCH_3	**5g**	3-OCH_3,4-OH	H	4-Br
5b	4-Cl	H	CH_3	**5h**	3-OCH_3,4-OH	H	4-Cl
5c	H	CH_3	OCH_3	**5i**	4-Cl	H	4-Br
5d	H	CH_3	CH_3	**5j**	H	CH_3	4-Br
5e	3-NO_2	H	CH_3	**5k**	H	CH_3	4-Cl
5f	4-OH	H	CH_3	**5l**	3-NO_2	H	4-Br

2.3. Biological activities

2.3.1. Structure activity relationship (SAR) of thiazole derivatives

The inhibitory potential of the synthesized thiazolyl ethanone derivatives **(5a-f)** and as well as thiazolyl hydrazines **(5g-h)** for *h*-TNAP as well as *h*-IAP was analyzed using human recombinant enzymes in both the cases (Table 2). Different substitutions and unsubstitution patterns were correlated with their ability to inhibit alkaline phosphatases. Such types of correlations help to develop SAR among the synthesized screened compounds. Levamisole is a thaizole derivative and has been reported as a known inhibitor of *h*-TNAP. Thiazole ring is the structural part of thiamine (Vitamin B_1), carboxylase, epothilones and macrocyclic thiopeptide antibiotics. This structural unit has broad range of biological activities including antimicrobial, anticonvulsant, antiviral, antibacterial, antituberculosis, antimalarial, anticancer, anti-inflammation, hypertension, schizophrenia and hypnotic. In the current study, thiazole derivatives were synthesized in order to find out more potent and selective antagonists of alkaline phosphatase. Among the synthesized derivatives, compounds **5a, 5e** and **5i** were found to be more potent against h-TNAP. The presence of nitro group at 3rd position of benzene ring in **5e**, made it highly potent against *h*-TNAP with IC_{50} of 0.17±0.01 µM which is 100 times more potent as compared to Levamisole with IC_{50} value of 25.2±1.90 µM. Structural comparison of compounds **5a** and **5f**, exhibited that methoxy group in 3-methoxybenzylidene ring, gave selectivity toward *h*-TNAP to **5a** with the IC_{50} value of 0.25±0.01 µM. **5b** exhibited inhibitory activity against both isoenzymes *h*-TNAP and *h*-IAP with IC_{50} 3.43±0.01 µM and 4.71± 0.03 µM, respectively, as compared to **5d** having no inhibitory activity. This activity is due to the presence of electron withdrawing group (chlorine) at *para*-position of the benzene ring. Compound **5f** was found to be more potent for *h*-IAP with IC_{50} value of 1.33±0.10 µM which is 75 times more potent than L-phenylalanine (IC_{50}: 100±3.00 µM). Mono-substitutions on benzene ring of the synthesized derivatives exhibited non-selectivity for both isozymes of

alkaline phosphatase. Such behavior of mono-substitution on benzene ring can be observed by comparing the structures of **5b, 5e, 5f** and **5l**. Removal of substitutions on benzene ring eliminated the inhibitory potential of molecules as can be noted from inhibitory activities of compounds **5c, 5d, 5j** and **5k**. Chlorine and bromine at *para*-position of the phenyl ring attached to thiazole the ring conferred **5h** and **5i** molecules selectivity towards *h*-TNAP with an IC_{50} values of 3.02±0.02 µM and 0.21±0.01 µM. **5j** and **5k** were found to be relatively less potent for both isozymes due to removal of substitution on phenyl ring, although their phenyl ring has halogens substitution. Incorporation of nitro group at *meta*-position of benzene ring and bromophenyl with thiazole ring in **5l** showed selective inhibition against *h*-TNAP with IC_{50} 1.38 ± 0.02 µM. Presence of chlorophenyl at position 4 of thiazole ring have no inhibitory activity against both isoenzymes *h*-TNAP and *h*-IAP as in **5k** molecule but incorporation of methoxy group at position 3 and OH group at position 4 of benzene ring show selective inhibition against *h*-TNAP with IC_{50} value of 3.02 ± 0.02 µM **(5h)**.

Table 2. APs inhibition of the screened thiazolyl ethanone **(5a-f)** and thiazolyl hydrazines derivatives **(5g-l)**

Compound	***h*-TNAP**	***h*-IAP**
	IC_{50}±SEM (µM) / % inhibition	
5a	0.25±0.01	12.34%
5b	3.43±0.01	4.71±0.03
5c	14.96%	3.15%
5d	11.22%	17.21%
5e	0.17±0.01	3.77±0.02
5f	4.56±0.03	1.33±0.10

5g	1.45±0.02	5.14±0.06
5h	3.02±0.02	10.46%
5i	0.21±0.01	11.23%
5j	11.10%	10.43%
5k	45.14%	11.67%
5l	1.38±0.02	12.16%
Levamisole	25.2±1.90	-
L-phenylalanine	-	100±3.00

2.3.2. Enzyme kinetics study for *h*-TNAP and *h*-IAP inhibition

Enzyme kinetics studies were performed to determine the mode of inhibition involves for *h*-TNAP and *h*-IAP. Most potent compounds were selected for such type of studies. 5e molecule exhibited competitive mode of inhibition for both *h*-TNAP and *h*-IAP. 0, 0.1, 0.5 and 1.0 µM concentrations were used for inhibitor **5e** and substrate concentration were 0, 12.5, 25, 50 and 100 µM. In addition, enzyme kinetic studies were also performed for **5i**, and compound exhibited mixed type of enzyme inhibition for *h*-TNAP **(Figure 2**).

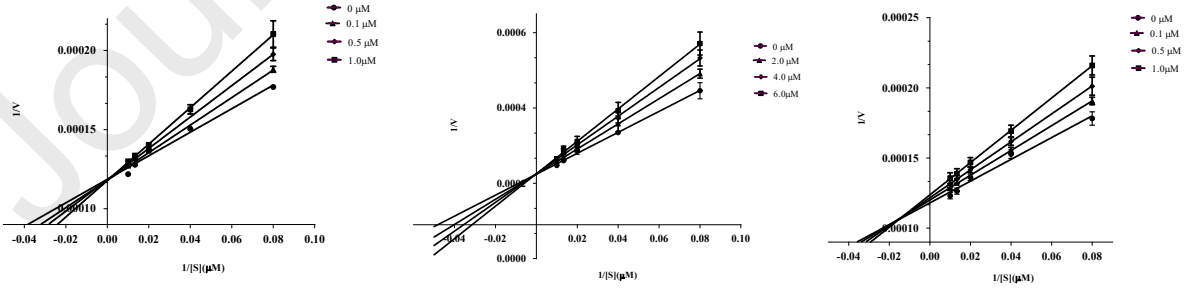

Figure 2. Double-reciprocal plots of the inhibition kinetics of *h*-TNAP by compounds **5e** (left) and of *h*-IAP by compound **5e** (middle) indicating competitive mode of inhibition. **5i** exhibited mixed type of inhibition (right) for *h*-TNAP.

2.3.4. Molecular modeling investigation

2.3.4.1. Molecular docking studies against human tissue non-specific alkaline phosphatase (*h*-TNAP)

The binding mechanism for the screened compounds against *h*-TNAP was validated by the binding mechanism of its positive control Levamisole (**Figure 3**). *In vitro* analysis found **5a**, **5e**, **5g**, **5i**, and **5l** as promising inhibitors of the *h*-TNAP protein, imitating the interactions of Levamisole. Zn^{2+}483 ion and His154 were involved in interaction with all the selected screened compounds. Arg167, Asp320, and His321 were the other prominent residues to interact with the screened compounds. Major interactions depicted were hydrogen bonding, π-π interactions, π-alkyl interactions and π-cation/anionic interactions between the residues and compounds. The compound **5a** showed additional interactions with Glu108 and Arg119 (**Figure 4**). Compound **5e** exhibited chemical interaction with the two Zn^{2+} ions, hydrogen bonding with His154, His321 and His437 residues, and π-π interaction with His324 residue (**Figure 5**). Compound **5g** interacted with a Zn^{2+} ion along with the His154, Arg167, Asp320, His324 and Thr436 residues (**Figure 6**). Compound **5i** was least reactive with the protein among the selected compounds exhibiting interactions with Zn^{2+} ion and Arg151, His154, His321 and His437 residues of the protein (**Figure 7**). Compound **5l** exhibited the usual interactions as displayed by other compounds of the group, involving interactions with both of Zn^{2+} ions, hydrogen bonding with His154 and His321 residues, π-anion interaction with arg167 and Asp320, π-π interactions with His324 and π-σ interactions with His434 residue in the active site of protein (**Figure 8**).

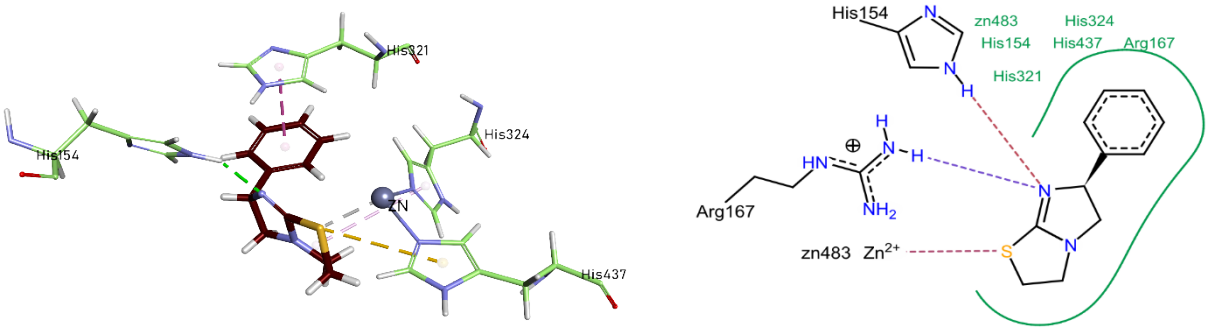

Figure 3: 3D & 2D interactions of Levamisole with ***h*-TNAP**

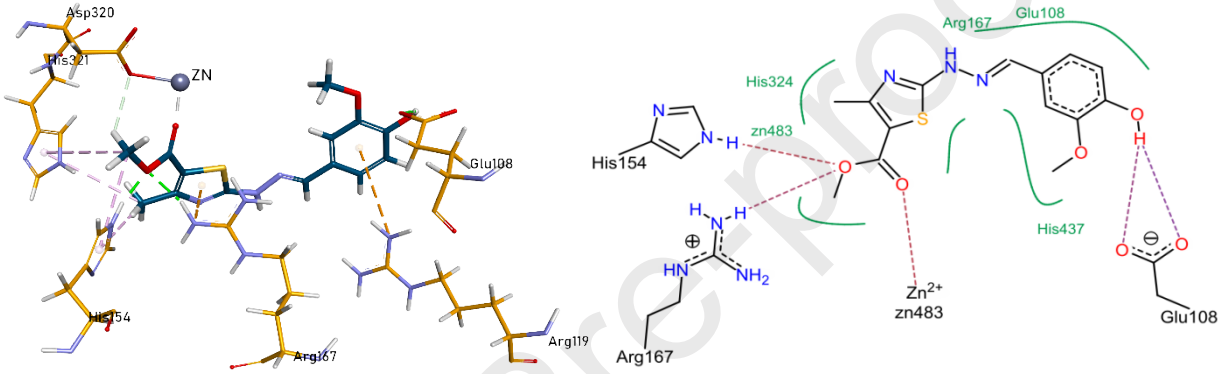

Figure 4: 3D & 2D interactions of **5a** with ***h*-TNAP**

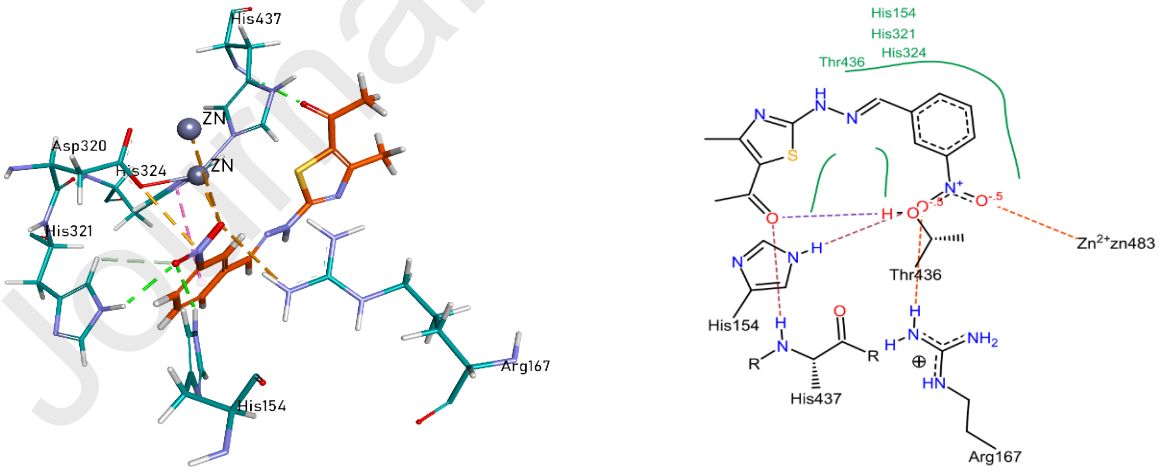

Figure 5: 3D & 2D interactions of **5e** with *h*-TNAP

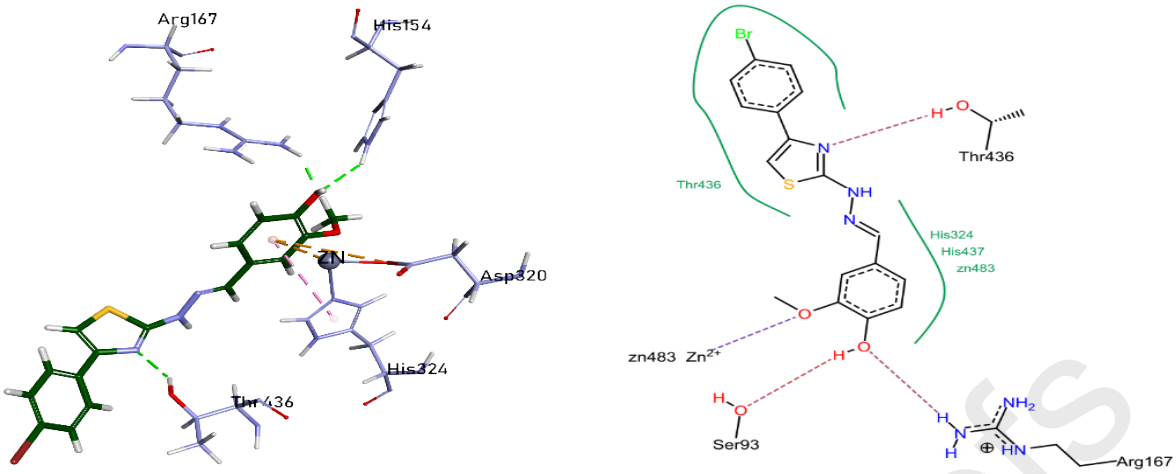

Figure 6: 3D & 2D interactions of **5g** with *h*-TNAP

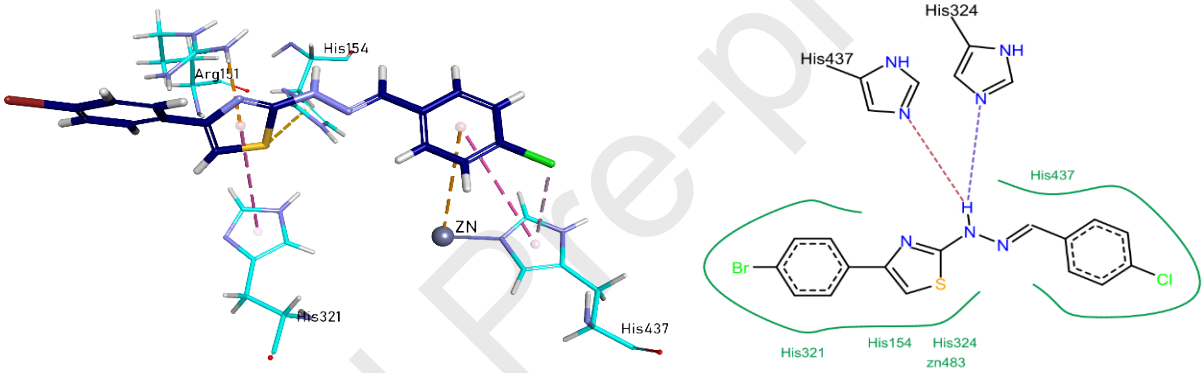

Figure 7: 3D & 2D interactions of **5i** with *h*-TNAP

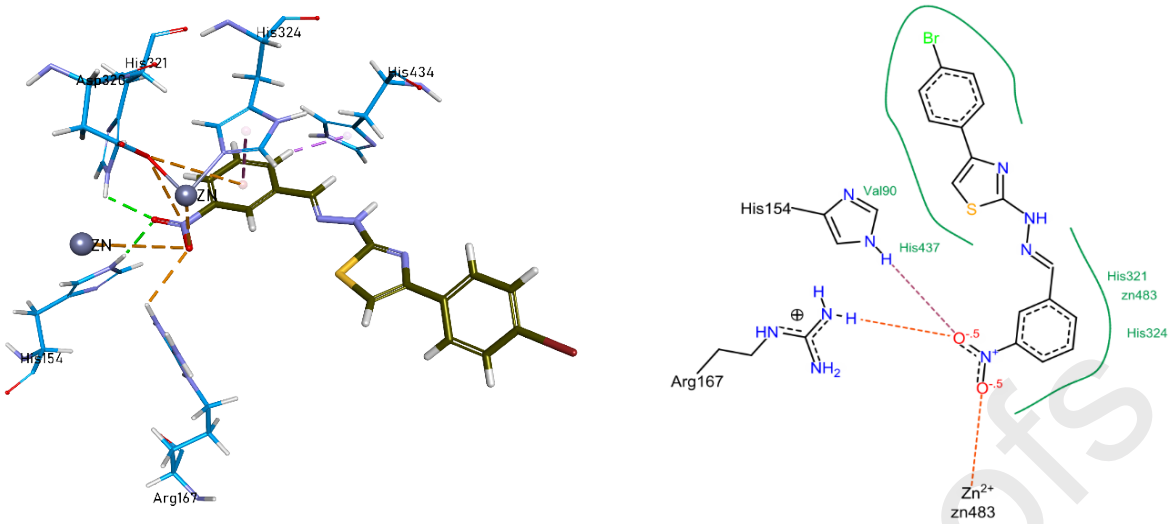

Figure 8: 3D & 2D interactions of **5l** with *h*-TNAP

2.3.4.2. Molecular docking studies against *h*-IAP

L-phenylalanine was initially docked into the *h*-IAP protein to find the binding site residues to validate the bindings for the test compounds. L-phenylalanine exhibited interactions with the two Zn^{2+} ions along with hydrogen bonding with Ser92, His153, His317, His358 and His432, while π- cationic interactions Asp42, Arg166, and Asp316 residues (**Figure 9**). *In vitro* analysis found **5e** and **5f** as potent inhibitors of the *h*-IAP protein, and the molecular docking provided the validation for it by imitating the interactions of L-phenylalanine. Both compounds, **5e** and **5f,** interacted with Zn^{2+} ion as illustrated in Figure **10** and **11**, respectively. Ser92 and His153 was involved in the formation of hydrogen bonding with all the compounds. Asp42, Arg166, Asp316, His317, His320 were among the common involved in the interactions with the test compounds as indicated by 2D and 3D interaction figures.

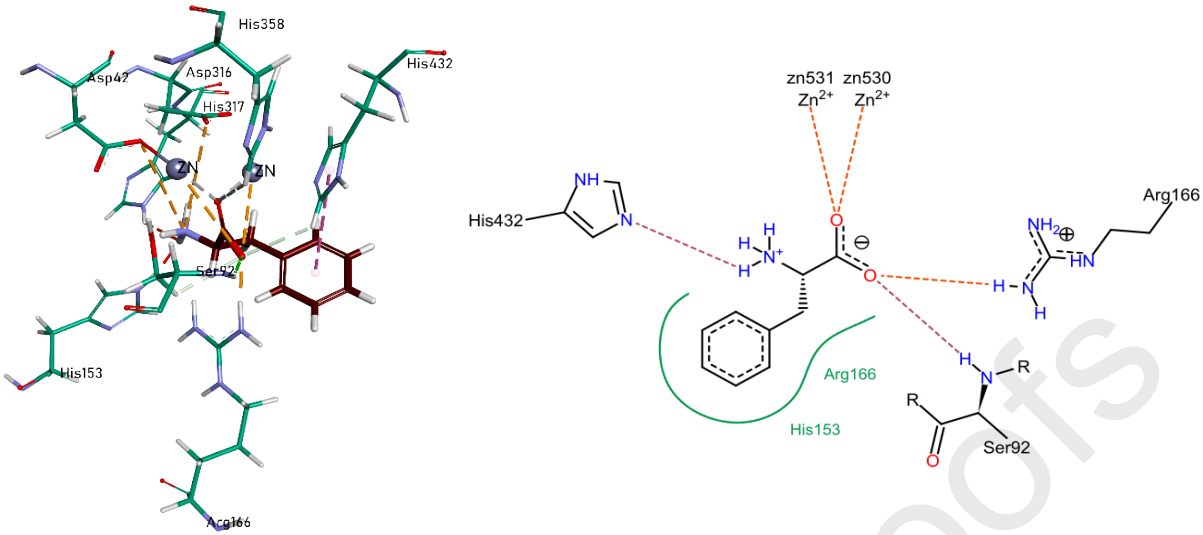

Figure 9: 3D & 2D interactions of L-phenylalanine with *h*-IAP

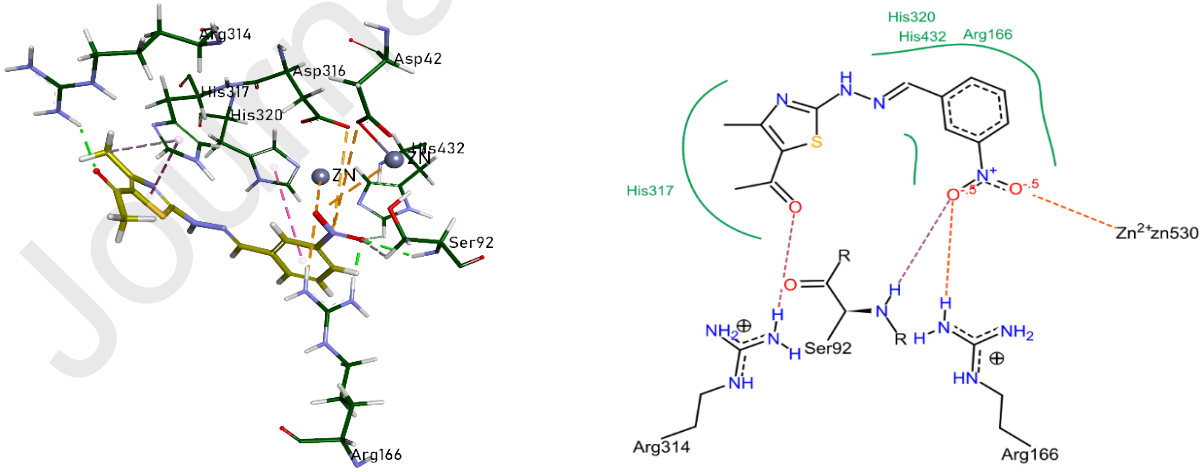

Figure 10: 3D & 2D interactions of **5e** with ***h*-IAP**

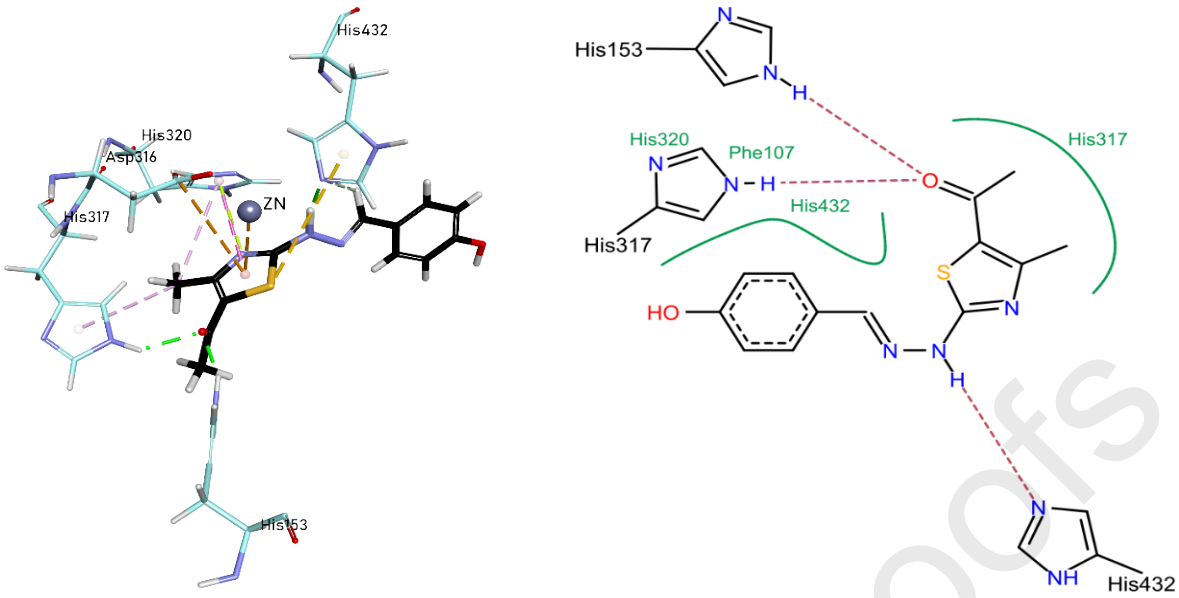

Figure 11: 3D & 2D interactions of **5f** with *h*-IAP

2.3.5. HYDE assessment of selective and potent compounds against *h*-IAP and *h*-TNAP

Pose selection criteria for selected potent compounds was further narrowed down by running HYDE affinity assessment tool of LeadIT and it served in the selection of appropriate binding mode. The FlexX score of the selective compounds and their binding free energy ΔG are given in table 3.

Table 3. FlexX score and binding free energy of ΔG of selected compounds

	Compound	FlexX score of the top-ranking pose	Binding free energy ΔG (kJ mol^{-1})
***h*-IAP**	**5e**	-30.4873	-0
	5f	-16.2262	-11
***h*-TNAP**	**5a**	-16.5975	-16
	5e	-29.6870	-5

	5g	-11.9777	-11
	5i	-9.0874	-10
	5l	-24.6684	-2

Molecular dynamic simulations

RMSD analysis

The RMSD values provide the information of overall stability of the protein and its complex with selected inhibitor when deviations need to calculate in the initial structure. As shown in Figure 12, three selected compounds (**5a**, **5e** and **5i**) are significantly stable and depicted less deviation within the range of 0.2 to 0.35 nm. The slight variation was consistent in the structure of *h*-TNAP alone, whereas, all the complex structures were found as significantly stable. The structure of **5e**+protein showed slight deviation around 8-10 ns while, **5a**+protein was found to show variability around 14 ns and remaining simulations were found stable. The structure of **5i**+protein was quite stable during the simulation time period. When the structure of IAP was monitored in apo and holo form, Cα backbone was prompted with an average of 0.3 nm for IAP and 0.28 nm for **5f**+protein. The stability was suggested with the overall RMSD of around 0.29 nm. A continuous negligible fluctuations were found throughout the simulation time. The results of both the protein structures showed the stability in terms of internal motion in systems.

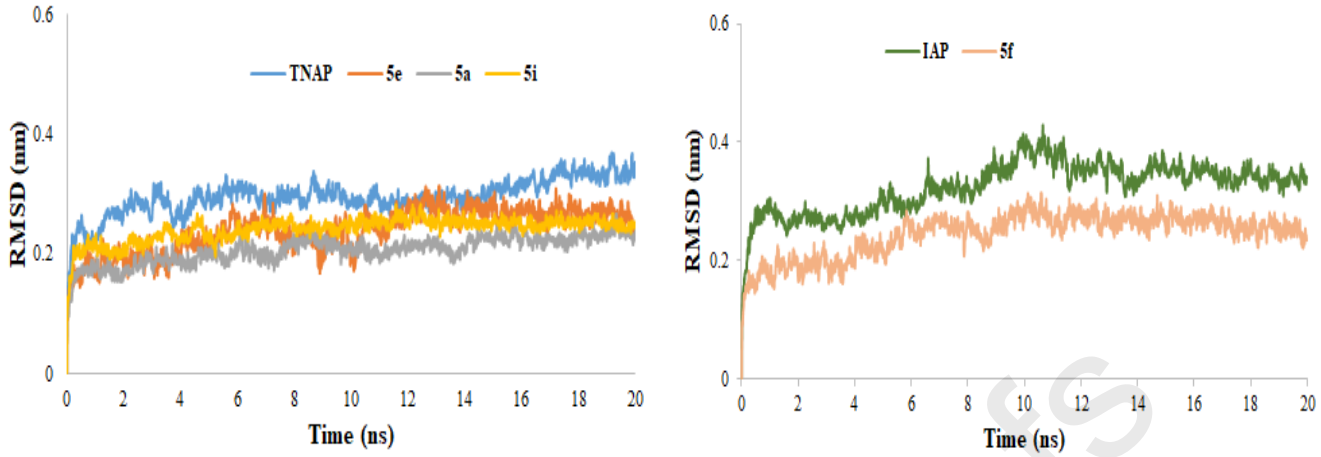

Figure 12. Root Mean Square Deviation (RMSD) of amino acid residues of *h*-TNAP and *h*-IAP protein during 20 ns MD-simulation run in the presence and absence of selected compounds

RMSF analysis

The knowledge of RMSF values also provide the information regarding the calculation that were carried out to investigate the flexibility of the protein structure in the presence and absence of selected compounds. As represented in Figure 13, both the systems presented significant pattern of fluctuations. However, the overall values of RMSF for TNAP and its complexes were around 0.25 nm, with slight increase in complex of 5i, which is around 0.3 nm. However, the IAP and its complex delineated the fluctuations around 0.3 nm as depicted in Figure 13. The region having loop was found to show slight fluctuations while active site region was significantly stable during the whole simulations time course. The results indicated that all the complexes result in stability of the system.

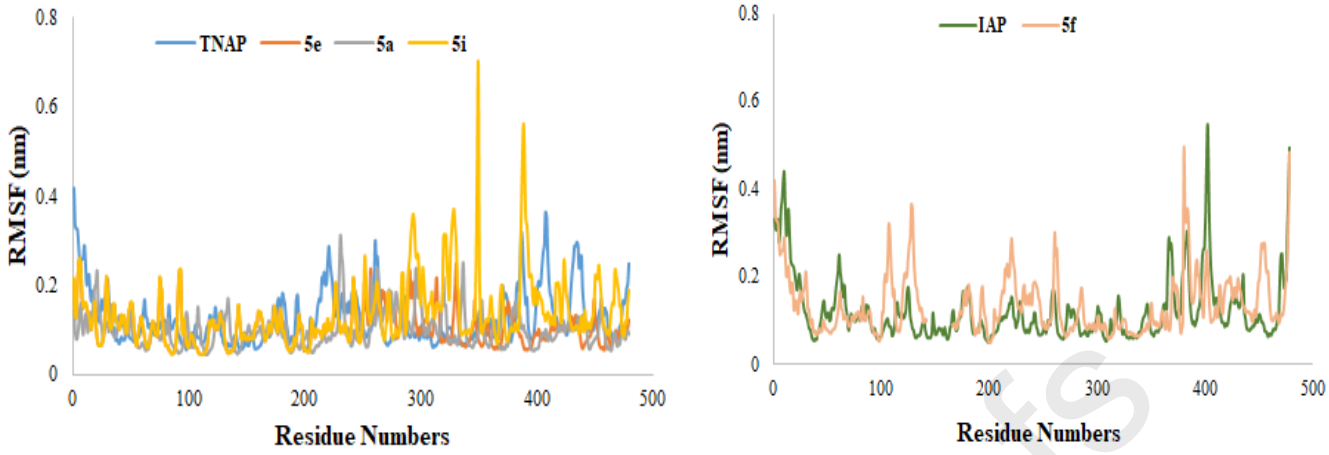

Figure 13. Root Mean Square Fluctuation (RMSF) of amino acid residues of *h*-TNAP and *h*-IAP protein during 20 ns MD-simulation run in the presence and absence of selected compound

Radius of gyration

The results of calculations carried out for the investigation of radius of gyration (Rg) presented the information about compactness of the system with time frame. Radius of gyration described the folding and unfolding of structure of protein in the presence and absence of selected inhibitors. The results were illustrated in Figure 14, suggesting that in comparison to TNAP alone, the complexes of **5a** and **5e** were more compact, while less compactness was shown by **5i**+TNAP complex. Figure 6 showed that an average score of Rg for TNAP and its complexes was 2.25 nm while for IAP and its complex, it was 2.2 nm. Our results depicted the compactness of systems throughout the simulations.

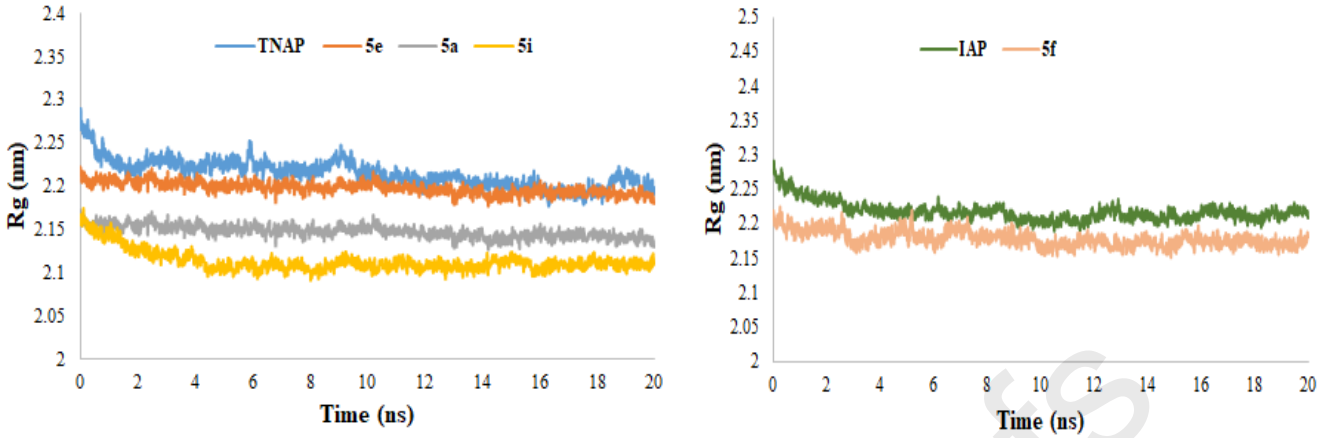

Figure 4. Radius of gyration (Rg) of amino acid residues of *h*-TsNAP and *h*-IAP protein structures during 20 ns MD-simulation run in the presence and absence of selected compounds

3. Conclusions

The current research study reports the successful synthesis and characterization of thiazolyl ethanone derivatives **(5a-f)** and thiazolyl hydrazines **(5g-l)**. The compounds were evaluated to determine their inhibitory potential against APs (*h*-TNAP and *h*-IAP). The compounds exhibiting most prominent inhibitory activity during *in vitro* analysis were subjected to molecular docking studies on *h*-TNAP and *h*-IAP, revealing the significant binding modes between the selected compounds and target proteins evincing inhibition of the respective enzymes.

4. Experimental

4.1. Chemistry

All the reagents involved were purchased from Sigma Aldrich and were used without any further purification. The glass ware was dried in an oven at 70 ℃ for one 60 minutes. Bruker Avance AVIII spectrometer was used to record the ^{1}H and ^{13}C nuclear magnetic resonance (NMR) spectra at 400 and 100 MHz respectively in deuterated DMSO-d_6 as a solvent and TMS as an internal reference. ^{1}H-NMR data is reported as δ values in ppm relative to residual

signals from deuterated solvents, while coupling constants are indicated by *J* in Hz. ^{13}C-NMR data were reported as position (δ) and assignment of the atom. The infrared spectra measured in wave numbers (cm^{-1}) was recorded using PerkinElmer Fourier transform infrared ATR spectrometer. Elemental analysis (C, H, N, S) was performed to determine the % presence of each element present. The progress of the reaction monitored using Thin-layer chromatography on silica gel 60 F254 precoated plates (0.25 mm) in a single spot/two solvent systems. Stuart MP-D melting point apparatus was used to determine the melting points of the synthesized compounds.

4.2. Synthesis of 2-benzylidenehydrazine-1-carbothioamide (3a-e)

For the synthesis of 2-benzylidenehydrazine-1-carbothioamide derivatives **(3a-e)** a reported methodology from literature with slight modifications was employed. For this purpose, appropriate benzaldehyde (1.20 mmol) was completely dissolved in distilled ethanol (05 mL) at room temperature and a drop of concentrated sulphuric acid was added as a catalyst. After 30 minutes of continuous stirring, a solution of thiosemicarbazide (1.20 mmol) prepared in distilled ethanol (10 mL) was dropwise added to the reaction mixture and the mixture was refluxed for next 120 minutes at 100 °C. TLC in a solvent system of *n*-hexane: ethyl acetate (4:1) was constantly employed to check the extent of reaction. After 120 minutes, the reaction mixture was cooled to room temperature which resulted in the formation of solid precipitates. The solid precipitates obtained were filtered, dried in an oven at 70 °C and recrystallized from ethanol to purify the corresponding 2-benzylidenehydrazine-1-carbothioamide derivatives **3(a-e)** [18-19].

4.2.1. 1-(4-Hydroxy-3-methoxybenzylidene)thiosemicarbazide (3a)

R_f= 0.28 (*n*-hexane: ethyl acetate, 4:1); m.p 222 °C; Mol. wt: 225.27; Orange powder; (Yield 73%): IR (Pure, cm^{-1}) ν: 3283.06 (NH_2), 3122.79 (NH), 3050.84 (sp^2 C-H), 2965.80 (sp^3 C-H), 1620.20 (HC=N), 1562.57, 1515.64, 1495.91 (Ar-C=C), 1154.32 (C=S); ^{1}H NMR (400 MHz,

DMSO-d_6, δ): 11.42 (b, s, 1H, NH), 9.19 (s, 1H, HC=N), 8.41 (b, s, 1H, OH), 8.12 (b, s, 1H, NH), 7.90 (b, s, 1H, NH), 7.53 (d, 1H, *J* = 7.80 Hz, Ar-H), 6.937 (d, 1H, *J* = 7.80 Hz, Ar-H), 6.75 (s, 1H, Ar-H), 3.79 (s, 3H, O-C-H); ^{13}C NMR (100 MHz, DMSO-d_6, δ): 178.08 (C=S), 148.32 (Ar), 146.40 (Ar), 139.91 (HC=N), 121.19 (Ar), 119.47 (Ar), 118.55 (Ar), 113.22 (Ar), 56.31 (O-C); Anal. Cald. For $C_9H_{11}N_3O_2S$: C, 47.99; H, 4.92; N, 18.65; S, 14.30; Found: C, 47.90; H, 4.95; N, 18.72; S, 14.10.

4.2.2. 1-(4-Chlorobenzylidene) thiosemicarbazide (3b)

R_f= 0.19 (*n*-hexane: ethyl acetate, 4:1); m.p 210 °C; Mol. wt: 213.69; Light yellow powder; (Yield 76%): IR (Pure, cm^{-1}) ν: 3180.38 (NH_2), 3106.65 (NH), 29621.65 (sp^2 C-H), 1596.64 (HC=N), 1575.19, 1519.73, 1489.17 (Ar-C=C), 1199.89 (C=S); ^{1}H NMR (`400 MHz, DMSO-d_6, δ): 10.26 (b, s, 1H, NH), 8.38 (b, s, 1H, NH), 7.89 (b, s, 1H, NH), 8.13 (s, 1H, HC=N), 7.69 (d, 2H, *J* = 8.10 Hz, Ar-H), 7.39 (d, 2H, J= 8.10 Hz, Ar-H); ^{13}C NMR (100 MHz, DMSO-d_6, δ): 181.43 (C=S), 143.30 (HC=N), 136.63 (Ar), 131.93 (Ar), 130.63 (Ar), 129.13 (Ar); Anal. Cald. For C_8H_8 ClN_3S: C, 44.97; H, 3.77; N, 19.66; S, 15.01; Found: C, 44.87; H, 3.81; N, 19.69; S, 15.1.

4.2.3. 1-(1-Phenylethylidene) thiosemicarbazide (3c)

R_f= 0.47 (*n*-hexane: ethyl acetate, 4:1); m.p 132-134 °C; Mol. wt: 193.27; Light yellow powder; (Yield 81%): IR (Pure, cm^{-1}) ν: 3368 (NH_2), 3229.10 (NH), 3174.54 (sp^2 C-H), 2969.93 (sp^3 C-H), 1639.57 (HC=N), 1578.56, 1548.86, 1499.54 (Ar-C=C), 1159.48 (C=S); ^{1}H NMR (400 MHz, DMSO-d_6, δ): 10.21 (b, s, 1H, NH), 8.28 (b, s, 1H, NH), 7.94 (b, s, 1H, NH), 7.92 (m, 2H, Ar-H), 7.389 (m, 3H, Ar-H), 2.30 (3H, C-H); ^{13}C NMR (100 MHz, DMSO-d_6, δ): 179.36 (C=S), 148.28 (C=N), 138.11 (Ar), 129.66 (Ar), 128.69 (Ar), 127.06 (Ar), 14.46 (C-H); Anal. Cald. For $C_9H_{11}N_3S$: C, 55.93; H, 5.74; N, 21.74; S, 16.59; Found: C, 55.80; H, 5.82; N, 21.80; S, 16.62.

4.2.4.1-(3-Nitrobenzylidene) thiosemicarbazide (3d)

R_f= 0.27 (*n*-hexane: ethyl acetate, 4:1); m.p 218 °C; Mol. wt: 224.24; Yellow powder; (Yield 81%): IR (Pure) ν: 3370.55 (NH_2), 3253.32 (NH), 3185.34, 2956.08 (sp^2 C-H), 1644.34 (HC=N), 1579.56, 1569.48, 1451.69 (Ar-C=C), 1120.34 (C=S); ^{1}H NMR (400 MHz, DMSO-d_6) δ: 11.08 (b, s, 1H, NH), 8.21 (b, s, 1H, NH), 7.98 (b, s, 1H, NH), 8.63 (s, 1H, Ar-H), 8.23 (d, 1H, *J*= 8.2 Hz, Ar-H), 8.19 (s, 1H, HC=N), 8.13 (d, 1H, *J* = 8.2 Hz, Ar-H), 7.70 (t, 1H, *J* = 8.0 Hz, Ar-H); ^{13}C NMR (100 MHz, DMSO-d_6) δ: 182.39 (C=S), 148.53 (Ar), 143.30 (HC=N), 135.33 (Ar), 134.73 (Ar), 129.83 (Ar), 124.13 (Ar), 123.43 (Ar); Anal. Cald. For $C_8H_8N_4O_2S$: C, 42.85; H, 3.60; N, 24.99; S, 14.30; Found: C, 42.80; H, 3.55; N, 24.95; S, 14.34.

4.2.5. 1-(4-Hydroxybenzylidene) thiosemicarbazide (3e)

R_f= 0.37 (*n*-hexane: ethyl acetate, 4:1); m.p 212-216 °C; Mol. wt: 195.24; Red powder; (Yield 82%): IR (Pure, cm^{-1}) ν: 3238.10 (NH_2), 3178.63 (NH), 1620.64 (HC=N), 1582.98, 1561.47, 1490.70 (Ar-C=C), 1159.67 (C=S); ^{1}H NMR (400 MHz, DMSO-d_6, δ): 10.20 (b, s, 1H, NH), 8.45 (b, s, 1H, OH), 8.24 (b, s, 1H, NH), 7.90 (b, s, 1H, NH), 8.43 (s, 1H, HC=N), 7.43 (d, 2H, *J* = 7.52 Hz, Ar-H), 6.83 (d, 2H, *J* = 7.52 Hz, Ar-H); ^{13}C NMR (100 MHz, DMSO-d_6, δ): 181.43 (C=S), 161.10 (Ar), 143.30 (HC=N), 130.90 (Ar), 126.43 (Ar), 116.30 (Ar); Anal. Cald. For $C_8H_9N_3O_3S$: C, 49.21; H, 4.65; N, 21.52; S, 16.42; Found: C, 49.12; H, 4.74; N, 21.42; S, 16.46.

4.3. Procedure for the synthesis of thiazolyl ethanones (5a-f) and thiazolyl hydrazines (5g-l)

The synthesis of 2-(2-benzylidenehydrazineyl) thiazole derivatives **(5a-l)** was achieved by slight modification of literature method. Briefly, an equimolar ratio of 2-benzylidenehydrazine-1-carbothioamide derivatives **(3a-e)** and phenacyl halides/1,3-dicarbonyl compounds were refluxed in distilled ethanol at 100 °C for 1-2 h. TLC was constantly employed to check the extent of reaction in a solvent system of *n*-hexane: ethyl acetate (4:1). Once the reaction was

completed, ethanol was removed under reduced pressure and the crude products obtained were recrystallized from ethanol at room temperature to purify the synthesized thiazole derivatives **(5a-l)** [18-19].

4.3.1. (*E*)-Methyl 2-(2-(4-hydroxy-3-methoxybenzylidene)hydrazinyl)-4-methylthiazole-5-carboxylate (5a)

R_f=0.36 (*n*-hexane: ethyl acetate, 4:1); m.p 244 ℃; Mol. wt: 321.35; Light yellow powder; (Yield 76%): IR (Pure) ν: 3201.32 (NH), 3098.65, 2958.67 (C=C-H), 2914.23, 2840.29 (-CH_3), 1625.73 (HC=N), 1592.34, 1514.56, 1498.52, 1446.15 (Ar-C=C), cm^{-1}; ^{1}H NMR (400 MHz, DMSO-d_6, δ): 11.08 (b, s, 1H, NH), 8.10 (s, 1H, HC=N), 7.10 (d, 1H, *J = 8.02 Hz,* Ar-H), 7.0 (s, 1H, Ar-H), 6.79 (d, 1H, *J = 8.02 Hz,* Ar-H); 3.88 (s, 3H, C-H), 3.74 (s, 3H, C-H), 2.48 (s, 3H, C-H); ^{13}C NMR (100 MHz, DMSO-d_6, δ): 170.52 (C=N), 166.34 (C=O), 156.78 (C=C), 151.56 (Ar), 148.66 (Ar), 143.43 (HC=N), 127.46 (Ar), 122.93 (Ar), 117.59 (Ar), 115.45 (C=C), 114.86 (Ar), 56.49 (O-C), 51.30 (O-C), 10.26 (C-H); Anal. Cald. For $C_{14}H_{15}N_3O_4S$: C, 52.33; H, 4.70; N, 13.08; S, 9.98; Found: C, 52.30; H, 4.68; N, 13.05; S, 9.96.

4.3.2. (*E*)-1-(2-(2-(4-chlorobenzylidene)hydrazinyl)-4-methylthiazol-5-yl)ethanone (5b)

R_f= 0.34 (*n*-hexane: ethyl acetate, 4:1); m.p 230 ℃; Mol. wt: 293.77; Yellow powder; (Yield 79%): IR (Pure) ν: 3212.46 (NH), 3052.86, 2921.73 (C=C-H), 2901.38, 2813.54 (-CH_3), 1613.24 (HC=N), 1595.66, 1548.84, 1552.58, 1477.16 (Ar-C=C), cm^{-1}; ^{1}H NMR (400 MHz, DMSO-d_6, δ): 11.19 (b, s, 1H, NH), 8.16 (s, 1H, HC=N), 7.64 (d, 2H, *J* = 8.10 *Hz,* Ar-H), 7.39 (d, 2H, *J* = 8.10 *Hz,* Ar-H), 2.56 (s, 3H, C-H); 2.49 (s, 3H, C-H); ^{13}C NMR (100 MHz, DMSO-d_6, δ): 196.89 (C=O), 170.56 (C=N), 156.78 (C=C), 144.30 (HC=N), 136.66 (Ar), 131.42 (Ar), 130.59 (Ar), 129.16 (Ar), 103.45 (C=C), 28.49 (C-H), 10.26 (C-H); Anal. Cald. For $C_{13}H_{12}ClN_3OS$: C, 53.15; H, 4.12; N, 14.30; S, 10.91; Found: C, 53.09; H, 4.15; N, 14.35; S, 10.89.

4.3.3. (*E*)-methyl 4-methyl-2-(2-(1-phenylethylidene)hydrazinyl)thiazole-5-carboxylate (5c)

R_f=0.52 (*n*-hexane: ethyl acetate, 4:1); m.p 123 °C; Mol. wt: 289.35; Light Yellow powder; (Yield 80%): IR (Pure) ν: 3192.50 (NH), 3051.73, 2961.57 (C=C-H), 2920.13, 2890.74 (-CH_3), 1629.38 (C=N), 1591.20, 1540.75, 1504.62, 1476.56 (Ar-C=C), cm^{-1}; ^{1}H NMR (400 MHz, DMSO-d_6, δ): 11.0 (b, s, 1H, NH), 7.67 (d, 2H, *J* = 8.2 *Hz,* Ar-H), 7.38 (t, 2H, *J = 8.2 Hz,* Ar-H), 7.10 (t, 1H, *J = 8.2 Hz,* Ar-H), 3.89 (s, 3H, C-H); 2.56 (s, 3H, C-H); 0.90 (s, 3H, C-H); ^{13}C NMR (100 MHz, DMSO-d_6, δ): 170.52 (C=N), 168.43 (C=N), 166.82 (C=O), 156.78 (C=C), 140.76 (Ar), 130.82 (Ar), 129.25 (Ar), 129.16 (Ar), 115.45 (C=C), 51.49 (O-C), 19.49 (C-H), 10.26 (C-H); Anal. Cald. For $C_{14}H_{15}N_3O_2S$: C, 58.11; H, 5.23; N, 14.52; S, 11.08; Found: C, 58.19; H, 5.20; N, 14.57; S, 11.08.

4.3.4. (*E*)-1-(4-methyl-2-(2-(1-phenylethylidene)hydrazinyl)thiazol-5-yl)ethanone (5d)

R_f=0.54 (*n*-hexane: ethyl acetate, 4:1); m.p°C; Mol. wt: 273.95; Yellow powder; (Yield 90%): IR (Pure) ν: 3352.56 (NH), 3092.48, 2912.67 (C=C-H), 2910.34, 2861.34 (-CH_3), 1632.12 (C=N), 1590.63, 1584.54, 1545.25, 1472.16 (Ar-C=C), cm^{-1}; ^{1}H NMR (400 MHz, DMSO-d_6, δ): 11.08 (b, s, 1H, NH), 7.56 (d, 2H, *J = 8.2 Hz,* A r-H), 7.19 (t, 2H, *J = 8.2 Hz,* Ar-H), 7.10 (t, 1H, , *J* = 8.2 Hz*,* Ar-H), 2.56 (s, 3H, C-H); 2.49 (s, 3H, C-H), 0.97 (s, 3H, C-H); ^{13}C NMR (100 MHz, DMSO-d_6, δ): 196.82 (C=O), 170.59 (C=N), 168.78 (C=N), 156.43 (C=C), 140.66 (Ar), 130.42 (Ar), 129.59 (Ar), 129.36 (Ar), 103.45 (C=C), 28.49 (C-H), 14.49 (C-H), 10.26 (C-H); Anal. Cald. For $C_{14}H_{15}N_3OS$: C, 61.51; H, 5.53; N, 15.37; S, 11.73; Found: C, 61.56; H, 5.55; N, 15.35; S, 11.74.

4.3.5 (*E*)-(1-(4-methyl-2-(2-(3-nitrobenzylidene)hydrazineyl)thiazol-5-yl)ethan-1-one (5e)

R_f=0.31(*n*-hexane: ethyl acetate, 4:1); m.p 255 °C; Mol. wt: 304.32; Yellow powder; (Yield 90%): IR (Pure) ν: 3262.27 (NH), 3125.48, 2954.63 (C=C-H), 2934.68, 2835.84 (-CH_3), 1632.74 (HC=N), 1593.64, 1543.84, 1525.28, 1470.72 (Ar-C=C), cm^{-1}; ^{1}H NMR (400 MHz,

DMSO-d_6, δ): 11.20 (b, s, 1H, NH), 8.64 (s, 1H, Ar-H), 8.26 (d, 1H, *J = 8.2 Hz,* Ar-H), 8.15 (d, 1H, *J = 8.2 Hz,* Ar-H), 8.14 (s, 1H, HC=N), 8.05 (t, 1H, *J = 8.0 Hz,* Ar-H), 2.56 (s, 3H, C-H); 2.49 (s, 3H, C-H); ^{13}C NMR (100 MHz, DMSO-d_6, δ): 196.90 (C=O), 170.59 (C=N), 156.78 (C=C), 148.56 (Ar), 143.46 (HC=N), 139.26 (Ar), 135.22 (Ar), 134.52 (Ar), 129.59 (Ar), 124.36 (Ar), 103.45 (C=C), 28.48 (C-H), 10.16 (C-H); Anal. Cald. For $C_{13}H_{12}N_4O_3S$: C, 51.31; H, 3.97; N, 18.41; S, 10.54; Found: C, 51.23; H, 3.95; N, 18.46; S, 10.59.

4.3.6. (*E*)-1-(2-(2-(4-hydroxybenzylidene)hydrazinyl)-4-methylthiazol-5-yl)ethanone (5f)

R_f=0.40 (*n*-hexane: ethyl acetate, 4:1); m.p 185 °C; Mol. wt: 275.33; Yellow powder; (Yield 70%): IR (Pure) ν: 3222.60 (NH), 3012.64, 2910.17 (C=C-H), 2902.13, 2806.14 (-CH_3), 1630.22 (HC=N), 1591.03, 1541.35, 1500.25, 1470.26 (Ar-C=C), cm^{-1}; ^{1}H NMR (400 MHz, DMSO-d_6, δ): 11.04 (b, s, 1H, NH), 8.12 (s, 1H, HC=N), 7.45 (d, 2H, *J = 7.52 Hz,* Ar-H), 6.86 (d, 2H, *J = 7.52 Hz,* Ar-H), 2.56 (s, 3H, C-H); 2.49 (s, 3H, C-H); ^{13}C NMR (100 MHz, DMSO-d_6, δ): 196.83 (C=O), 170.53 (C=N), 160.65 (Ar), 156.78 (C=C), 144.48 (HC=N), 130.42 (Ar), 126.59 (Ar), 116.36 (Ar), 103.45 (C=C), 28.49 (C-H), 10.26 (C-H); Anal. Cald. For $C_{13}H_{13}N_3O_2S$: C, 56.71; H, 4.76; N, 15.26; S, 11.65; Found: C, 56.62; H, 4.79; N, 15.32; S, 11.69.

4.3.7. (*E*)-4-((2-(4-(4-bromophenyl)thiazol-2-yl)hydrazono)methyl)-2-methoxyphenol (5g)

R_f=0.27 (*n*-hexane: ethyl acetate, 4:1); m.p 165 °C; Mol. wt: 404.28; Yellow powder; (Yield 73%): IR (Pure) ν: 3328.93 (OH), 3246.90 (NH), 3087.46, 2974.59 (C=C-H), 2924.28 (-CH_3), 1620.54 (HC=N), 1593.68, 1567.26, 1536.76, 1470.78 (Ar-C=C), cm^{-1}; ^{1}H NMR (400 MHz, DMSO-d_6, δ): 11.0 (b, s, 1H, NH), 8.09 (s, 1H, HC=N), 7.52 (d, 2H, *J = 8.20 Hz,* Ar-H), 7.48 (d, 2H, *J = 8.20 Hz,* Ar-H), 7.10 (s, 1H, Ar-H), 7.04 (d, 1H, *J = 8.02 Hz,* Ar-H), 6.90 (d, 1H, *J = 8.02 Hz,* Ar-H), 6.65 (s, 1H, C=C-H), 4.50 (b, s, 1H, OH), 3.75 (s, C-H); ^{13}C NMR (100

MHz, DMSO-d_6, δ): 171.80 (C=N), 151.50 (Ar), 148.19 (C=C), 148.10 (Ar), 143.42 (HC=N), 132.85 (Ar), 132.42 (Ar), 129.74 (Ar), 127.42 (Ar), 123.29 (Ar), 123.15 (Ar), 117.43 (Ar), 114.43 (Ar), 100.43 (C=C), 56.50 (O-C); Anal. Cald. For $C_{17}H_{14}BrN_3O_2S$: C, 50.50; H, 3.49; N, 10.39; S, 7.93; Found: C, 50.45; H, 3.54; N, 10.43; S, 7.93.

4.3.8. 1-(4-Hydroxy-3-methoxybenzylidene)-2-(4-(4-chlorophenyl)thiazol-2-yl) hydrazine (5h)

R_f=0.30 (*n*-hexane: ethyl acetate, 4:1); m.p 130 ℃; Mol. wt: 359.83; Yellow powder; (Yield 70%): IR (Pure) ν: 3317.85 (OH), 3219.57 (NH), 3052.56, 2989.34 (C=C-H), 2943.19 (-CH_3), 1632.48 (HC=N), 1567.26, 1520.63, 1479.20 (Ar-C=C), cm^{-1}; ^{1}H NMR (400 MHz, DMSO-d_6, δ): 11.04 (b, s, 1H, NH), 8.10 (s, 1H, HC=N), 7.54 (d, 2H, *J = 8.20 Hz,* Ar-H), 7.48 (d, 2H, *J = 8.20 Hz,* Ar-H), 7.32 (s, 1H, Ar-H); 7.10 (d, 1H, *J = 8.02 Hz,* Ar-H), 6.70 (d, 1H, *J = 8.02 Hz,* Ar-H), 6.60 (s, 1H, C=C-H), 4.99 (b, s, 1H, OH), 3.76 (s, 3H, C-H); ^{13}C NMR (100 MHz, DMSO-d_6, δ): 171.86 (C=N), 151.56 (Ar), 148.51 (C=C), 147.99 (Ar), 143.18 (HC=N), 134.48 (Ar), 131.86 (Ar), 129.40 (Ar), 128.93 (Ar), 127.40 (Ar), 122.90 (Ar), 117.56 (Ar), 114.89 (Ar), 100.48 (C=C), 56.50 (O-C); Anal. Cald. For $C_{17}H_{14}ClN_3O_2S$: C, 56.74; H, 3.92; N, 11.68; S, 8.91; Found: C, 56.69; H, 3.96; N, 11.74; S, 8.95.

4.3.9. (*E*)-4-(4-bromophenyl)-2-(2-(4-chlorobenzylidene)hydrazinyl)thiazole (5i)

R_f= 0.39 (*n*-hexane: ethyl acetate, 4:1); m.p 135 ℃; Mol. wt: 392.70; Yellow powder; (Yield 74%): IR (Pure) ν: 3276.10 (NH), 2987.59 (C=C-H), 1623.45 (HC=N), 1597.56, 1568.26, 1537.62, 1479.08 (Ar-C=C), cm^{-1}; ^{1}H NMR (400 MHz, DMSO-d_6, δ): 11.20 (b, s, 1H, NH), 8.20 (s, 1H, HC=N), 7.65 (d, 2H, *J = 8.10 Hz,* Ar-H), 7.50 (d, 2H, *J = 8.2 Hz,* Ar-H), 7.38 (d, 2H, *J = 8.20 Hz,* Ar-H); 7.30 (d, 2H, *J = 8.10 Hz,* Ar-H), 6.64 (s, 1H, C=C-H); ^{13}C NMR (100 MHz, DMSO-d_6, δ): 171.80 (C=N), 146.50 (C=C), 143.22 (HC=N), 134.44 (Ar), 131.76 (Ar), 130.85 (Ar), 129.42 (Ar), 129.24 (Ar), 129.12 (Ar), 128.95 (Ar), 123.05 (Ar), 100.49 (C=C);

Anal. Cald. For $C_{16}H_{11}BrClN_3S$: C, 48.94; H, 2.82; N, 10.70; S, 8.17; Found: C, 48.89; H, 2.84; N, 10.67; S, 8.20.

4.3.10. 1-(4-(4-Bromophenyl) thiazol-2-yl)-2-(1-phenylethylidene) hydrazine (5j)

R_f= 0.48 (*n*-hexane: ethyl acetate, 4:1); m.p 250 °C; Mol. wt: 372.78; Yellow powder; (Yield 80%): IR (Pure) ν: 3246.90 (NH), 3054.24, 2935.15 (C=C-H), 2924.47 (-CH_3), 1603.83 (C=N), 1518.44, 1484.99, 1472.65, 1445.10 (Ar-C=C), cm^{-1}; ^{1}H NMR (400 MHz, DMSO-d_6, δ): 11.02 (b, s, 1H, NH), 7.54 (d, 2H, *J = 8.2 Hz,* Ar-H), 7.41 (d, 2H *J = 8.2 Hz,* Ar-H); 7.36-7.10 (m, 5H, Ar-H), 6.64 (s, 1H, C=C-H), 0.95 (s, 3H, C-H); ^{13}C NMR (100 MHz, DMSO-d_6, δ): 171.80 (C=N), 168.39 (C=N), 148.50 (C=C), 134.44 (Ar), 132.25 (Ar), 132.20 (Ar), 131.29 (Ar), 129.95 (Ar), 129.71 (Ar), 128.95 (Ar), 123.22 (Ar), 100.49 (C=C), 13.80 (C-H); Anal. Cald. For $C_{17}H_{14}BrN_3S$: C, 54.85; H, 3.79; N, 11.29; S, 8.61; Found: C, 54.80; H, 3.84; N, 11.32; S, 8.62.

4.3.11. (*E*)-4-(4-chlorophenyl)-2-(2-(1-phenylethylidene)hydrazinyl)thiazole (5k)

R_f= 0.45 (*n*-hexane: ethyl acetate, 4:1); m.p 160 °C; Mol. wt: 327.83; Yellow powder; (Yield 86%): IR (Pure) ν: 3283.54 (NH), 3105.28, 2969.63 (C=C-H), 2919.88, 2850.74 (-CH_3), 1637.24 (C=N), 1598.48, 1556.14, 1505.23, 1475.75 (Ar-C=C), cm^{-1}; ^{1}H NMR (400 MHz, DMSO-d_6, δ): 11.09 (b, s, 1H, NH), 7.56 (d, 2H, *J = 8.2 Hz,* Ar-H), 7.49 (d, 2H, *J = 8.2 Hz,* Ar-H), 7.36-7.10 (m, 5H, Ar-H), 6.64 (s, 1H, C=C-H), 0.96 (s, 3H, C-H); ^{13}C NMR (100 MHz, DMSO-d_6, δ): 171.82 (C=N), 168.34 (C=N), 148.28 (C=C), 134.43 (Ar), 134.26 (Ar), 134.16 (Ar), 131.10 (Ar), 129.42 (Ar), 129.25 (Ar), 128.95 (Ar), 128.93 (Ar), 100.49 (C=C), 13.85 (C-H); Anal. Cald. For $C_{17}H_{14}ClN_3S$: C, 62.28; H, 4.30; N, 12.82; S, 9.78; Found: C, 62.22; H, 4.35; N, 12.80; S, 9.82.

4.3.12. (*E*)-4-(4-bromophenyl)-2-(2-(3-nitrobenzylidene)hydrazinyl)thiazole (5l)

R_f=0.40 (*n*-hexane: ethyl acetate, 4:1); m.p 228 °C; Mol. wt: 403.25; Yellow powder; (Yield 90%): IR (Pure) ν: 3183.59 (NH), 3061.51, 2917.35 (C=C-H), 1580.05 (HC=N), 1526.82, 1474.25, 1446.20, 1422.80 (Ar-C=C), cm^{-1}; ^{1}H NMR (400 MHz, DMSO-d_6, δ): 11.20 (b, s, 1H, NH), 8.25 (s, 1H, HC=N), 8.20 (d, 2H, *J = 8.2 Hz,* Ar-H), 8.05 (d, 2H, *J = 8.2 Hz,* Ar-H), 7.76 (d, 1H, *J = 8.2 Hz,* Ar-H); 7.54 (t, 1H, *J = 8.2 Hz,* Ar-H), 7.50 (d, 1H, *J = 8.2 Hz,* Ar-H), 7.04 (s, 1H, Ar-H), 6.64 (s, 1H, C=C-H);^{13}C NMR (100 MHz, DMSO-d_6, δ): 171.82 (C=N), 148.42 (Ar), 148.28 (HC=N), 146.52 (C=C), 134.43 (Ar), 134.24 (Ar), 132.86 (Ar), 132.43 (Ar), 129.85 (Ar), 129.70 (Ar), 124.95 (Ar), 123.43 (Ar), 123.14 (Ar), 100.49 (C=C); Anal. Cald. For $C_{16}H_{11}BrN_4O_2S$: C, 47.66; H, 2.75; N, 13.89; S, 7.95; Found: C, 47.54; H, 2.81; N, 13.85; S, 7.99.

4.4. *In vitro* biological assay

4.4.1. Cells transfection

Transfection of plasmids that encodes *h*-TNAP and *h*-IAP was done by method previously reported [20]. 24 hours before transfection, COS-7 cells were seeded until the cells gain 80-90% confluency. Cells were incubated for 5 to 6 hours at 37^{O}C after adding serum free Dulbecco's modified eagle's medium (DMEM) containing 6 µg of plasmid DNA and 24 µl of Lipofectamine reagent. After 48 hours of incubation, media was removed and normal growth media containing 20% FBS was added. Extraction and quantification of expressed protein were done by Bradford method. Protein fraction was stored at -80 ^{O}C as aliquots that were made in 7.5% of glycerol.

4.4.2. Alkaline phosphatase Inhibition assay

Analysis of synthesized compounds was conducted for the inhibitory activity against specific enzymes according to previously reported protocol after slight modification [21]. Recombinant

h-TNAP and *h*-IAP enzymes were used. Luminescent substrate CDP-Star® was used having chemical name of Disodium 2-chloro-5 [4-methoxyspiro (1,2-dioxetane-3,2′ {5-chlorotricyclo (3.3.1.13.7) deacon]} -4-yl] -1-phenyl phosphate. Beginning of all, working solutions were made by using dilution buffer. Working solutions of enzymes were prepared in dilution buffer of diethanol amine (DEA) with the concentration of 250 mM. In the first step, 20µl of enzyme solution (5 µg/mL for *h*-TNAP and 3.335 µg/mL for *h*-IAP) and 10 µL of test compound (final compound conc. 200 µM, and DMSO less than 2% V/V conc.) were added in each well of 384 wells white plate. Incubated for 5-7 minutes at 37 °C and after that luminescence signals were noted through microplate reader. Then, 20 µL of substrate (CDP -Star®) was added to each well with the final concentration of 177µM of *h*-IAP and 105.2 µM of *h*-TNAP. After 7 to 10 minutes incubation again readings for luminescence signals were taken. At the end, percentage of enzyme inhibition was measured and compounds having inhibitory activity more than 50% were analyzed further for the measurement of IC_{50} value. Software utilized for this analysis was PRISM 5.0, [GraphPad, San Diego, California, USA.].

4.4.3. Molecular docking studies

4.4.3.1. Selection of the protein structures and preparation of ligands

Homology modeled structures of *h*-TNAP and *h*-IAP, previously generated and reported by our research group were used to perform the molecular docking studies [22]. The proteins were protonated and minimized using Molecular Operating Environment (MOE) [23]. The selected compound structures were prepared by MOE builder, and their energy was minimized by an appropriate force field. *h*-TNAP and *h*-IAP models binding validation was done with the positive standards used in the biological assay. MOE site finder was used for the selections of binding site of these receptors, keeping the catalytic zinc ions in the center of the active site. After initial validation, molecular docking of the selected ligands was carried out.

4.4.3.2. Docking experiment

Molecular docking studies were performed on LeadIT (BioSolveIT GmbH, Germany) by utilizing default parameters, for the selected compounds as well as the reference standards (used in in-vitro assay) [24]. The most promising docked pose was selected for each ligand and it was further analyzed by the HYDE assessment tool. The 3D interactions of the poses were examined using Discovery Studio Visualizer [25].

Molecular dynamic simulations

For MD simulations, protein manipulation and protonation were made with the help of GROMOS96 force field having the 43a1 parameter set. The GROMACS simulation packages, 5.1.4 were used for the MD simulations using previously used methods [26-28]. To observe the effect of potent inhibitors against respective protein, an apo system (protein having no ligand) was constructed for each protein. Parametrization of selected compound was carried out by online PRODRG servers [29]. MOE [23] and VMD [30] was used for the visualization of trajectories. After the energy minimization of system, two sequential NVT (100 ps) and NPT (100 ps) runs were performed for equilibration of system. The resulting ensembles were subjected to 20 ns MD simulations with a time step of 2 fs. Periodic boundary conditions were applied during MD simulations. All NVT and NPT ensembles used the Berendsen thermostat and the Parrinello-Rahman barostat for temperature (approx. 302-303 K) and pressure coupling (approx. 1.01 bar), respectively. Cut-off radios of 10 Å and smooth Particle Mesh Ewald protocol were observed for long-range method. Root mean square deviation, fluctuations and radius of gyration of protein was plotted using XMGRACE v5.1.19 [31].

Conflict of interests

The author(s) declare that they have no conflict of interests.

Acknowledgements

H.A. acknowledges an Indigenous scholarship from Higher Education Commission of Pakistan as a financial support. J.I. is thankful to the Higher Education Commission of Pakistan for the financial support through Project No.Ph-V-MG-3/Peridot/R&D/HEC/2019. J.S. received support from the Natural Sciences and Engineering Research Council of Canada (NSERC; RGPIN-2016-05867).

References:

1. Shen, C., Li, X., Rasooly, A., Guo, L., Zhang, K., & Yang, M. (2016). A single electrochemical biosensor for detecting the activity and inhibition of both protein kinase and alkaline phosphatase based on phosphate ions induced deposition of redox precipitates. *Biosensors and Bioelectronics*, *85*, 220-225.
2. M. Boztaş, Y. Çetinkaya, M. Topal, İ. Gülçin, A. Menzek, E. Şahin, M. Tanc, C.T. Supuran, Synthesis and carbonic anhydrase isoenzymes I, II, IX, and XII inhibitory effects of dimethoxy-bromophenol derivatives incorporating cyclopropane moieties. *Journal of Medicinal Chemistry*, 58 (2), 2015, 640-650.
3. A. Yıldırım, U. Atmaca, A. Keskin, M. Topal, M. Çelik. İ. Gülçin, C. T Supuran, N-Acylsulfonamides strongly inhibit human carbonic anhydrase isoenzymes I and II. *Bioorg. Med. Chem.*, 23(10), 2015, 2598-2605.
4. T. Artunc, A. Menzeka, P. Taslimi, I. Gulcin, C. Kazaz, E. Sahina, Synthesis and antioxidant activities of phenol derivatives from 1,6-bis(dimethoxyphenyl)hexane-1,6-dione. *Bioorg.Chem.*, 100, 2020, 103884
5. al-Rashida, M., Ejaz, S. A., Ali, S., Shaukat, A., Hamayoun, M., Ahmed, M., & Iqbal, J. (2015). Diarylsulfonamides and their bioisosteres as dual inhibitors of alkaline phosphatase

and carbonic anhydrase: structure activity relationship and molecular modelling studies. *Bioorg. Med. Chem.*, *23*(10), 2435-2444.

6. Tang, Z., Chen, H., He, H., & Ma, C. (2019). Assays for alkaline phosphatase activity: progress and prospects. *TrAC Tren. Anal. Chem.*, 113, 32-43
7. Grodner, B., &Napiórkowska, M. (2017). Characterization and inhibition studies of tissue nonspecific alkaline phosphatase by aminoalkanol derivatives of 1, 7-dimethyl-8, 9-diphenyl-4-azatricyclo [5.2. 1.02, 6] dec-8-ene-3, 5, 10-trione, new competitive and non-competitive inhibitors, by capillary electrophoresis. *Journal of pharmaceutical and biomedical analysis*, *143*, 285-290.
8. Lallès, J. P. (2019). Biology, environmental and nutritional modulation of skin mucus alkaline phosphatase in fish: A review. *Fish & shellfish immunology*.
9. Hassan, G. S., El-Messery, S. M., Al-Omary, F. A., & El-Subbagh, H. I. (2012). Substituted thiazoles VII. Synthesis and antitumor activity of certain 2-(substituted amino)-4-phenyl-1, 3-thiazole analogs. *Bioorg. Med. Chem.Lett.*, *22*(20), 6318-6323.
10. T Chhabria, M., Patel, S., Modi, P., & S Brahmkshatriya, P. (2016). Thiazole: a review on chemistry, synthesis and therapeutic importance of its derivatives. *Curr. Top. Med. Chem.*, *16*(26), 2841-2862.
11. Bondock, S., Fadaly, W., &Metwally, M. A. (2010). Synthesis and antimicrobial activity of some new thiazole, thiophene and pyrazole derivatives containing benzothiazole moiety. *Eur. J. Med. Chem*., *45*(9), 3692-3701.
12. Al-Saadi, M. S., Faidallah, H. M., & Rostom, S. A. (2008). Synthesis and Biological Evaluation of Some 2, 4, 5-Trisubstituted Thiazole Derivatives as Potential Antimicrobial and Anticancer Agents. *Archiv der Pharmazie, 41*(7), 424-434.

13. Deng, X. Q., Song, M. X., Wei, C. X., Li, F. N., & Quan, Z. S. (2010). Synthesis and anticonvulsant activity of 7-alkoxy-triazolo-[3, 4-b] benzo [d] thiazoles. *Med. Chem.*, *6*(5), 313-320.

14. Kalkhambkar, R. G., Kulkarni, G. M., Shivkumar, H., & Rao, R. N. (2007). Synthesis of novel triheterocyclic thiazoles as anti-inflammatory and analgesic agents. *Eur. J. Med. Chem*., *42*(10), 1272-1276.

15. Jaishree, V., Ramdas, N., Sachin, J., & Ramesh, B. (2012). In vitro antioxidant properties of new thiazole derivatives. *Journal of Saudi Chemical Society*, *16*(4), 371-376.

16. Holla, B. S., Malini, K. V., Rao, B. S., Sarojini, B. K., & Kumari, N. S. (2003). Synthesis of some new 2, 4-disubstituted thiazoles as possible antibacterial and anti-inflammatory agents. *Eur. J. Med. Chem*., *38*(3), 313-318.

17. I. Khan, S. Zaib, A. Ibrar, N.H. Rama, J. Simpson, J. Iqbal Synthesis, crystal structure and biological evaluation of some novel 1, 2, 4-triazolo [3, 4-b]-1, 3, 4-thiadiazoles and 1, 2, 4-triazolo [3, 4-b]-1, 3, 4-thiadiazines, *Eur. J. Med. Chem*.,78(2014), pp.167-177.

18. Reddy G.M., Garcia J.R., Reddy V.H., de Andrade A.M., Camilo A., Jr., Ribeiro R.A.P., de Lazaro S.R. Synthesis, antimicrobial activity and advances in structure-activity relationships (SARs) of novel tri-substituted thiazole derivatives. (2016). *Eur. J. Med. Chem. 123*, 508–513.

19. Chemical Computing Group's Molecular Operating Environment (MOE) MOE 2019.0201.

20. LeadIT version 2.3.2; BioSolveIT GmbH, Sankt Augustin, Germany, 2017, www.biosolveit.de/LeadIT

21. Dassault Systèmes BIOVIA, Discovery Studio Modeling Environment, Release 2017, San Diego: Dassault Systèmes, 2016.

22. Ferreira, R. J., Ferreira, M. J., Daniel, U., dos Santos, V. J. (2012). A. Insights on P-Glycoprotein's Efflux Mechanism Obtained by Molecular Dynamics Simulations. *J. Chem. Theory Comput. 8*, 1853-1864.

23. Mathew, B., Haridas, A., Ucar, G., Baysal, I., Adeniyi, A. A., Soliman, M. E., Joy, M., Mathew, G. E., Lakshmanan, B., Jayaprakash. V. (2016). Exploration of chlorinated thienyl chalcones: A new class of monoamine oxidase-B inhibitors. *Int. J. Biol. Macromolec. 91*, 680-695.

24. Özgeris, B., Göksu, S., Köse, L. P., Gülcin, I., Salmas, R. E., Durdagi, S., Tümer, F., Supuran, C. T. (2016). Acetylcholinesterase and carbonic anhydrase inhibitory properties of novel urea and sulfamide derivatives incorporating dopaminergic 2-aminotetralin scaffolds. *Bioorg. Med. Chem. 24*, 2318-2329.

25. Schüttelkopf, A. W., van Aalten. D. M. F. (2004). PRODRG: a tool for high-throughput crystallography of protein-ligand complexes. *Acta Crystallogr. Sect. D: Biol. Crystallogr. 60,* 1355-1363.

26. Humphrey, W., Dalke, A., Schulten, K. (1996). VMD: Visual Molecular Dynamics. *J. Mol. Graphics, 14*, 33-38.

27. Turner. P. (2005). XMGRACE, Version 5.1. 19. Center for Coastal and Land-Margin Research, Oregon Graduate Institute of Science and Technology, Beaverton.

Conflict of Interest

The authors declare that they have no conflict of interest.

Graphical abstract:

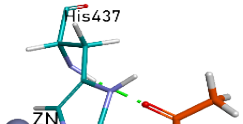

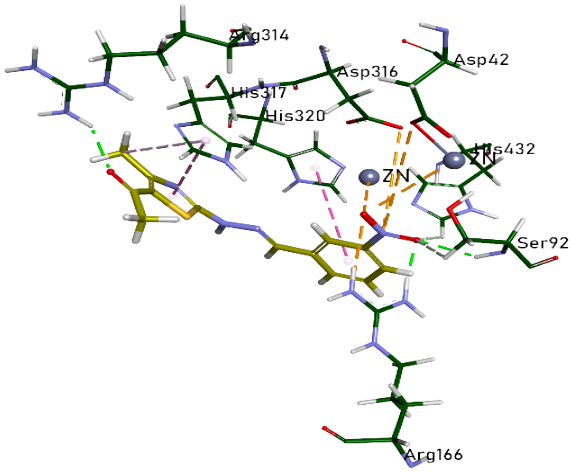

Binding interactions of compound ***5e*** in *h*-IAP (left) and compound ***5e*** *h*-TNAP (right) showing competitive mode of inhibition in both the enzymes

Highlights

- New thiosemicarbazides (**3a-3e)** were heterocyclized with 1,3-dicarbonyls to afford thiazoles (**5a-f**) and with phenacyl halides to furnish the thiazoles (**5g-l**).
- The functionalized thiazoles (**5a-l**), were subjected to *h*-TNAP and *h*-IAP assay and **5e** and **5f** were identified as most active molecules.
- Molecular docking of **5e** and **5f** on *h*-TNAP and *h*-IAP to explore the binding interactions was carried out
- Molecular dynamic simulations were carried out to investigate the overall stability of protein in apo and holo state.